# 行政院國家科學委員會專題研究計畫　期中精簡報告

## 由共振腔結構決定非線性雷射動力學研究(2/3)

計畫類別： 個別型計畫
計畫編號： NSC91-2112-M-009-040-
執行期間： 91 年 08 月 01 日至 92 年 07 月 31 日
執行單位： 國立交通大學光電工程研究所

計畫主持人： 謝文峰
共同主持人： 程思誠

報告類型： 精簡報告

處理方式： 本計畫可公開查詢

中　華　民　國 92 年 5 月 12 日

附件一

# 行政院國家科學委員會補助專題研究計畫 □成果報告 X期中進度報告

**由共振腔結構決定非線性雷射動力學研究(2/3)**

計畫類別：X 個別型計畫　　□ 整合型計畫
計畫編號：NSC 91-2112-M-009-040-
執行期間： 91 年 08 月 01 日至 93 年 07 月 31 日

計畫主持人：謝文峰
共同主持人：
計畫參與人員：

成果報告類型(依經費核定清單規定繳交)：X 精簡報告　□完整報告

本成果報告包括以下應繳交之附件：
□赴國外出差或研習心得報告一份
□赴大陸地區出差或研習心得報告一份
□出席國際學術會議心得報告及發表之論文各一份
□國際合作研究計畫國外研究報告書一份

處理方式：除產學合作研究計畫、提升產業技術及人才培育研究計畫、列管計畫及下列情形者外，得立即公開查詢
□涉及專利或其他智慧財產權，□一年□二年後可公開

查詢

執行單位：國立交通大學光電工程研究所

中　華　民　國 92 年 05 月 06 日

行政院國家科學委員會專題研究計畫期中進度報告

# 由共振腔結構決定的非線性雷射動力學研究(2/3)

Resonator configuration dependent nonlinear laser dynamics (2/3)

計畫編號：NSC 91-2112-M-009-040-
執行期限：91 年 8 月 1 日至 92 年 7 月 31 日
主持人：謝文峰教授　　國立交通大學光電工程研究所

## 一、中文摘要

在本報告中我們藉著改變腔內總色散，在虛光闌克爾鎖模鈦藍寶石雷射中觀察到諧頻鎖模與多脈衝之操作模式，我們可以觀察到二階、三階、甚至四皆知諧頻鎖模以及脈衝間距由飛秒到奈秒之多重脈衝。上述之雷射操作狀態是依雷射之操作波長、頻寬、脈寬、和脈衝功率為總群色散之函數關係作分類。引進額外之損失項於增益動態分析，我們可以完全解釋所觀察到之雷射物理現象。

**關鍵詞**：雷射、共振腔、光渾沌現象、固態雷射。

## Abstract

We report the observation of harmonic mode locking and multiple pulse operations in a soft-aperture Kerr-lens mode-locked Ti:sapphire laser by varying the total intra-cavity dispersion. Second, third, and fourth order harmonic mode locking as well as multiple pulsing with interpulse separation ranging from femtosecond to nanosecond are observed. The laser is characterized in these regimes in terms of wavelength, bandwidth, pulsewidth, average and peak powers as functions of group velocity dispersion. By introducing a loss difference term into gain dynamic analysis, we conclude that gain depletion and recovery mechanisms are responsible for the underlying physics of current observations.

Keywords: Laser, Resonator, Optical Chaos, Solid-State Laser.

## 二、緣由與目的

Resulting from the soliton-like pulse shaping effect via the interplay between the self phase modulation (SPM) and the group velocity dispersion (GVD), generation of ultra-short pulses have been achieved in Kerr-lens mode-locked (KLM) Ti:sapphire lasers [1-4]. Because of extremely high nonlinear effects, it is not surprising that the pulse splitting and multiple pulse operation can be observed in these laser systems besides the normal mode locking (NML). A single pulse per round trip splits into two

or three pulses with fs spacing had been observed in a soft-aperture KLM (SAKLM) Ti:sapphire laser [2]. The pulse-splitting is attributed to side-lobe pulse separation by the interplay of the negative GVD and SPM in the laser cavity. In a hard-aperture KLM (HAKLM) Ti:sapphire laser, other than the fs-split pulses, multiple pulse operations with asymmetric ns-splitting were also observed [3]. It is explained by the enhanced nonlinear interaction caused by two counter-propagating pulses coinciding within the active medium to stabilize the interpulse spacing equal to the round trip time between the active medium and one of the output couplers.

With an ion-implanted semiconductor as the saturable-absorber mirror [4], double to quadruple pulses were observed in a passive mode-locked Ti:sapphire laser. The interpulse spacing was obtained ranging from several hundred fs to several ns without reliably reproducible spacing [4] when the GVD was decreased below a critical value. The results were directly compared with the simulation from the Ginzburg-Landau equation. Recently, harmonic mode locking generated in the passive mode-locked fiber ring lasers were reported and attributed to soliton interaction by means of acoustic effects [5-7]. Harmonic operation of a passively mode-locked short-cavity $Cr^{4+}$:YAG laser with one, two, and three pulses in the cavity has been demonstrated [8] for various values of total cavity GVD. By increasing the intracavity power of a passively harmonic mode-locked erbium/ytterbium laser with short cavity, up to 11 pulses in the cavity with nearly equal pulse-to-pulse temporal spacing has also been observed [9]. An analytic model based on the interaction between the pulses through the transient gain depletion and recovery dynamics in the gain medium [10] was proposed to explain these phenomena. Similar gain dynamics had already been successfully applied to explain harmonic mode locking in an external cavity semiconductor laser by adjusting the injection current [11]. It contains two-section multiple quantum well structures of which one providing gain and the other acting as the slow saturable absorber.

We report, for the first time to our knowledge, the observation of second, third, and fourth order harmonic mode locking in a SAKLM Ti:sapphire laser without saturable absorber. Multiple pulsing with interpulse separation ranging from femtosecond to nanosecond was also observed. The mode-locked states are distinguished into three regions and characterized in terms of wavelength, time bandwidth product (TBP), pulse width, average and peak powers as function of group velocity dispersion. By introducing a loss difference of the split pulses into theoretical analysis of gain depletion and recovery model [10], we find that multiple pulses with unequal spacing between the pulses can take place in addition to the harmonic mode locking which occurs when the loss difference is neglected,

## 三、研究方法與步驟

The experiment was carried out by a SAKLM Ti:sapphire laser with a near symmetric cavity as shown in Fig. 1. The SAKLM Ti:sapphire laser consists of a 9-mm long Brewster-cut Ti:sapphire rod (Ti:0.1%, FOM>150), two curved mirrors (M1 and M2) of 10-cm radius of curvature tilted by $10^{o}$ angle, and two flat mirrors--a 99% high reflector M4 and a 95% output coupler M3. Both the distances between M2 and M4 as well as M1 and M3 are adjusted around 74 cm to form a near symmetric configuration. A pair of Brewster-angled SF10 prisms separated by 27 cm is inserted between M1 and M3 for dispersion compensation that allows for femtosecond pulses generation. The prism pair is mounted on the translation stage to finely adjust negative GVD, which can be determined from Ref. [12]. Thus the total intra-cavity GVD (β") could be estimated by taking the positive dispersion of the crystal into account. The total cavity length is approximate 160 cm that corresponds to the repetition rate of 93.3 MHz or round trip time of 10.7 ns. An all-line continuous wave (CW) Ar ion laser (Coherent, Innova 300) was employed to pump the Ti:sapphire crystal via a plano-convex lens with the focal length of 12.7 cm. Two fast photodiodes (Electro-Physics Technology ET-2000 with rise time 100 ps) together with an oscilloscope (LeCroy 94504A, bandwidth 300 MHz) and an rf-spectrum analyzer (HP-8560E) are employed to observe the pulse train and its corresponding power-spectrum. A collinear autocorrelator combined with a GaAsP photodiode (Hamamtsu G117) acting as two-photon absorption detector [13] is constructed to achieve interferometric autocorrelation measurement of pulse waveforms. Finally, the optical-spectra were measured by using an optical spectrum analyzer (Ophir wavestar).

## 四、結果與討論

### *A. Regimes for normal mode locking, harmonic mode locking, and multiple pulsing*

As our previous experimental results [14], the SAKLM operation usually occurs at the fractional degenerate cavity con.gurations [15] with peculiar mode patterns consisting of superposition of the fundamental mode with low-order degenerate transverse modes. In this experiment, we translated the curved mirror M2 along the optic axis of cavity to search for pertinent cavity con.guration so that the SAKLM operation was achieved. Throughout the experiment, the pumping power and the insertion width of the .rst prism P1 into laser beam were kept to the value of 4.5 W and 0.37 mm. Subsequently, we moved the translation stage to change the insertion width of the second prism P2 into laser beam in order to change the negative GVD. Besides the NML, the laser could also be operated with second, third, and fourth order harmonic mode locking as well as stable multiple pulsing whose interpulse separation ranges from femtosecond to nanosecond.

On the basis of our observation, we divided mode-locked operation into three regions as a function of the total intra-cavity GVD (β") that is shown later in Figs. 6 and 7. In region I, β" is less than - 2250 $fs^2$ where only the NML is observed. Further increasing β" to the region II (- 2250 $fs^2$ < β" < -1950 $fs^2$), the system exhibits two possible states either in the NML or in second harmonic mode locking (SHML) whose repetition period becomes one-half of the cavity round trip time. Occasionally, with a certain β" in this region, unstable pulse-splitting with ps spacing is found that would slowly turn into the SHML. In region III of which β" > -1950 $fs^2$, multiple pulses with unequal nanosecond interpulse spacing were observed and sometimes third harmonic mode locking (THML) or even fourth harmonic mode locking (FHML) pulses could be observed at the far limit of this region. Mostly, multiple pulses with unequal nanosecond interpulse spacing were found immediately as laser operated in this region. However, the NML may also be found initially and maintained in few-seconds to minutes and eventually developed into stable multiple pulse operation. Therefore, fewer data of the NML can be recorded in region III of Figs. 6 and 7 before they developed into pulse-splitting. We can also block the laser to destroy the mode locking at multiple pulsing and initial the mode locking again for observing the NML. In Fig. 2, we show a typical interference autocorrelation trace (solid line) for the NML measured at β" ~ -2768 $fs^2$ about 60 fs pulsewidth that is fitted with the $sech^2(-1.76\ t/t_0)$ curve (dot line). The inset is the corresponding optical-spectrum with center wavelength at 825 nm and bandwidth of 12.4 nm by fitting with a $sech^2$ profile (bold line). The autocorrelator can also be employed to resolve sub-picosecond pulse-splitting. In Figs. 3(a) and (b), the autocorrelation trace exhibits pulse-to-pulse separation of 210 and 475 fs, respectively. As mentioned before [16,17], the phase difference between two pulses can be gained from the optical-spectrum with the relation $\phi = 2\pi(\omega_0 - \omega_1)/(\omega_1 - \omega_2)$. Here $\omega_0$ is the central frequency of the fitting $sech^2$ curve and $w_1$ and$w_2$ are the closest frequency to $\omega_0$. It reveals that the relative phases of the split pulses in Fig. 3(a) and (b) are $\pi$ and $\pi/2$, respectively. Under different operation conditions, the change of relative phase of pulses around p and 0 between pulses was also seen.

We have observed multiple pulses with the interpulse separation larger than 10 ps which could not be observed by our autocorrelator but could be displayed by the oscilloscope. The double pulses in Fig. 4(a) shows split spacing of 2.6 ns with its corresponding rf-spectrum in Fig. 4(b). Similarly, we observed stable three asymmetric ns-spacing pulses as shown in Fig. 4(c) whose rf-spectrum is in Fig. 4(d). In addition, the four pulses having pulse spacing 1.8, 1.3, and 2.6 ns followed by a 5-ns blanking are shown in Fig. 4(e) with corresponding spectrum in Fig. 4(f). It is worth to mention that the relative spacing and amplitude for multiple pulses could be altered at the different total intra-cavity GVD while we change the insertion length of

the second prism.

The pulse trains together with their corresponding rf-spectra for the NML, SHML, THML, and FHML are shown in Fig. 5, respectively. The period of pulse train for the NML shown in Fig. 5(a) is equal to cavity round trip time with four harmonics of longitudinal beating in corresponding rf-spectrum [see Fig. 5(b)]. In Fig. 5(c), the SHML state has two pulses within a round trip in which its spectrum shows the first and third harmonics being suppressed below the noise level (-70 dB) in Fig. 5(d) to verify that the pulse train is highly periodic. Similarly, highly periodic and suppressing of the first, second and fourth harmonics below the noise level in Figs. 5(e)-(f) displays the laser is at the THML state. The FHML appears in the system with only the fourth harmonic as shown in Fig. 5(h). However, due to the limited bandwidth of our 300-MHz oscilloscope, which is smaller than the 373-MHz repetition rate of the FHML state, large pulse-to-pulse fluctuation is recorded in Fig. 5(g). The variations of the measured average output power (solid symbols), pulsewidth (open symbols), and the intra-cavity peak power versus the total intra-cavity GVD for the NML, SHML and double pulses are shown in Figs. 6(a) and (b). In Fig. 6(a) the average power (solid squares) and pulsewidth (open squares) of the NML are about 271 mW and 84 fs, respectively, at the largest |β”| and then suddenly decrease to around 200 mW and 55 fs at β” ~ -2760 $fs^2$ in region I. Pulsewidth decrease accompanied with intra-cavity peak power increase [shown as solid squares in Fig. 6(b)] is due to better GVD compensation by the prism pair. In addition, the operation wavelength is continuously red shifted to the maximum excursion at 827 nm where the time bandwidth product (TBP) is near the transform-limit of 0.318 forβ” ~ -2760 fs2 as shown in Fig. 7. Then the average power of the NML keeps almost constant until region III with a relatively small deviation of 10 mW or 5% and the pulsewidth is approximately 53 fs. Since the 5.35 ns-separated pulses in region II can extract more energy from the active medium in a round trip, the SHML pulse (solid circle in Fig. 6(a)) shows higher average output power about 310 mW with 62 fs pulsewidth at $b"_2$ ~ -2220 $fs^2$. However, the fact of two pulses in one round trip together with the broader pulsewidth for the SHML in comparison with the NML causes the pulses at the SHML (solid circle) in Fig. 6(b) having smaller intra-cavity peak power than that at the NML (solid square). Thus the peak power of single pulse at the SHML declines to 0.54 MW (almost a half of the NML one). Generally, pulses at the NML state have a little higher value of the TBP near 0.39 and recover at the state of the SHML as shown in Fig. 7. In region III of Figs. 6 and 7, two kinds of double pulses are found in our laser system and labeled with triangle and diamond symbols. One (triangle symbol) shows near equal spacing between pulses on the oscilloscope like that observe in the SHML. However, its odd numbers of longitudinal beatings on rf-spectrum are still above the noise level

(-70 dB) revealing a little unequal interpulse spacing between pulses. The others with asymmetric nanosecond splitting spacing between pulses are labeled diamond symbol whose time traces are shown in Fig. 4(a). Double pulses in region III of Fig. 6(a) reveals a little shorter pulsewidth than the SHML pulses in region II, but their bandwidth become a little broader to cause the value of the TBP slightly larger than the SHML in Fig. 7. In addition, the average power of double pulses in Fig. 6(a) tends to drop as β" declining in region III to cause the peak power fall in Fig. 6(b). The operation wavelength of the pulses gradually decreases throughout the region II and III in Fig. 7 and the lasing wavelength at either the state of the SHML or double pulses is longer than that at the NML state.

### *B. Explanations for harmonic mode locking and multiple pulsing*

Pulse-splitting with regular interspacing or harmonic mode locking has been observed in passive mode-locked fiber laser that was explained by the acoustic effect created by the electrostriction in fiber [5-7]. The refractive index change caused by the acoustic effect for a 9-mm Ti:sapphire crystal is too small to cause harmonic mode locking in such a laser. We therefore try to use the transient depletion and recovery of gain dynamics [10], which has been successfully applied to the passive harmonic mode-locked semiconductor [11], $Cr^{4+}$:YAG [8], and Er/Yb fiber lasers [9] with saturable absorber to explain the observed harmonic mode-locked phenomena. As the pulse goes through a gain medium, the gain saturation induced group velocity drift may drive the pulse toward the higher gain [10].

Assuming, initially, two pulses per round trip with unequal separation, one of pulses with larger depleted gain will experience larger group-velocity drift relative to the other pulse. After repeating this process in the cavity, two pulses will become equal spacing in one round trip time if the gain recovery time is longer than the cavity round-trip time and the depleted gain is much smaller than the total net gain [10]. Similar analysis can also be applied for N (N > 2) pulses to result in equal interpulse spacing among a cavity round trip period or termed Nth-harmonic mode locking. Since the recovery time of the Ti:sapphire about 2.5 μs is much longer than cavity round trip time of 10.6 ns, the observed harmonic mode locking in our experiment can be explained by the aforementioned gain dynamics. Two, three, and four pulses with asymmetric ns-spacing were observed similar to that reported in the HAKLM Ti:sapphire laser [6] in which two pulses with temporal separation equal to the round trip time from the laser rod to the output coupler and back will collide in the Kerr medium.

Because the two linear arms of our laser system are near equal, if aforementioned pulse colliding mechanism does play the role, the SHML should always be observed and ns-split pulse will not be seen. Furthermore, for the THML, three pulses traveling around the cavity are separated by 1/3 of round trip time ($T_0$). Assume that one of the pulses is located at the Kerr medium at some moment, the other two pulses will be located ahead and behind of

$1=3T_0$, they will never collide one another in the active medium. In most cases the interpulse spacing is arbitrary such as that shown in Fig. 4(a) where interpulse spacing is different from the SHML of 5.4 ns or the THML of 3.6 ns. These phenomena observed in our system cannot be explained in terms of pulse colliding within the active medium, and therefore some other mechanisms should be considered in order to explain our results.

The wavelength dependent gain profile [18] of Ti:sapphire crystal and reflectance of curved mirrors are shown in Fig. 8. We can see that the maximum value of Ti:sapphire gain profile [18] is located around 800 nm and the high reflection coating of our mirrors has a bandwidth from 780 to 880 nm. The pulses experience the higher instantaneous gain in region II where the operation wavelength is around 802-810 nm. Thus, the dynamic gain introduces enough repulsive force (group velocity drift) to push the ps-split pulses to equal interpulse spacing and form the SHML in region II. However, for multiple pulsing in region III, the operation wavelength of the laser is less than 802 nm (Fig. 7) so that the loss increases due to abruptly decrease of the reflectance of the mirrors (Fig. 8). This is consistent with experimental observation as shown in region III of Fig. 6 where the average powers of pulses reduce. Assuming two ps-split pulses with slightly different peak intensities, the stronger pulse will experience larger SPM and higher loss than the other.

By introducing an excess loss of the individual pulse into the instantaneous gain to modify the theoretical analysis of gain depletion and recovery model as described in [10], we are able to obtain analytical solution of multiple pulses with unequal spacing occurring in a cavity. The detailed derivation is shown in Appendix A. The difference of interpulse separations in Eq. (A.8) displays an additional term that depends on the loss difference between pulses as compared with [10, Eq. (12)], where it always converges to zero without the loss difference between pulses. In our system, the round trip loss without considering the excess loss introduced by finite bandwidth of the mirrors is about 3% such that the instantaneous gain $g_i$ is 0.321 in order to balance the loss. For the measured interpulse separations 2.6 and 8.1 ns within a round trip, as shown in Fig. 4(a), which corresponds to 5.4 ns difference of interpulse separations, we calculated the loss difference between two pulses is only 1%. This value is quite reasonable for the center wavelength below 795 nm where the mirror reflectance shows strong wavelength dependent (see Fig. 8) to result in ns-pulse-splitting as shown by diamond symbol in Fig. 7. Similar analysis can also be applied for N (N > 2) pulses per round trip with equal interpulse spacing to result in the Nth-harmonic mode locking or multiple pulses with unequal separation.

## 五、自我評估

由於我們在第一期添購之作為鈦藍寶石雷射之幫浦源倍頻 Nd:$YVO_4$ 雷射部份之尾款，因為有教育部卓越計劃之幫助先行墊付。今年度我們變更計劃採購氬離子

雷射管和量測單模雷射波長所需之干涉儀。這儀器將有助於我們了解去年報告中提出之新型之所謂多回徑本徵模，或多光腰模之真正物理內涵，這將會是新年度(本計劃第三期)計劃最主要之研究方向。本報告中之諧頻鎖模與脈衝分裂現象，也是由我們多年來研究有關共振腔結構相關之動態不穩定所造成。除了以上之報告外，在本年度計畫下，到目前為止共發表九篇 SCI 論文，其中有關雷射動力學研究計三篇，其他六篇為有關光電材料之物理性質研究，成果還算不錯。

## 六、結論

We have observed multiple pulses per round trip occurring in a soft-aperture Kerr-lens mode-locked Ti:sapphire laser. By varying the total intra- cavity dispersion, equally spaced harmonic operation and unequally spaced pulses with separation ranging from femtosecond to nanosecond can be found. The harmonic mode locking is observed for the first time to our knowledge without adding saturable absorber that could be reasonably explained by the gain dynamics. An investigation of the laser operated in these regimes in terms of wavelength, bandwidth, pulsewidth, average and peak powers as functions of group velocity dispersion shows that the operating wavelength of unequally spaced pulses is shorter than that of equally spaced pulses. In addition, the information of gain profile for amplifying medium and wavelength-dependent reflectance for mirrors suggest pulses with different wavelength as well as bandwidth may undergo different gain and loss. We then introduce a loss difference of the pulses into gain dynamic analysis and find that the steady state solution of multiple pulses with unequal spacing between the pulses exist in addition to harmonic mode locking. The solution expects that only 1% loss difference is sufficiently to cause 2.6 ns of pulse-splitting.

## 七、參考文獻

[1] C. Spielmann, P.F. Curley, T. Brabec, T. Brabec, F. Krausz, IEEE J. Quantum Electron. 30 (1994) 1100-1114.

[2] C.-Y. Wang, W. Zhang, K.F. Lee, K.M. Yoo, Opt. Commun. 137 (1997) 89-92.

[3] M. Lai, J. Nicholson, W. Rudolph, Opt. Commun. 142 (1997) 45-49.

[4] M.J. Lederer, B. Luther-Davies, H.H. Tan, C. Jagadish, N.N. Akhmediev, J.M. Soto-Crespo, J. Opt. Soc. B 16 (1999) 895-904.

[5] A.B. Grudinin, D.J. Richardson, D.N. Payne, Electron. Lett. 29 (1993) 1860~1861.

[6] S. Gray, A.B. Grudinin, W.H. Loh, D.N. Payne, Opt. Lett. 20 (1995) 189~191.

[7] A.B. Grudinin, S. Gray, J. Opt. Soc. Am. B 14 (1997) 144~154.

[8] B.C. Collings, K. Bergman, W.H. Knox, Opt. Lett. 22 (1997) 1098–100.

[9] B.C. Collings, K. Bergman, W.H. Knox, Opt. Lett. 23 (1998) 123–25.

[10] J. Nathan Kutz, B.C. Collings, K. Bergman, W.H. Knox, IEEE J. Quantum Electron. 34 (1998) 1749-1757.

[11] S. Sanders, A. Yariv, J. Paslaski, J.E. Ungar, H.A. Zarem, Appl. Phys. Lett. 58 (1991) 681–683.

[12] K.-H. Lin, W.-F. Hsieh, J. Opt. Soc. Am. B 13 (1996) 1786–1793.

[13] J.K. Ranka, A.L. Gaeta, A. Baltuska, M.S. Pschenichnikov, D.A. Wiersma, Opt. Lett. 22 (1997) 1344–1346.

[14] J.H. Lin, M.D. Wei, W.F. Hsieh, H.H. Wu, J. Opt. Soc. Am. B 18 (2001) 1069–1075.

[15] H.H. Wu, W.F. Hsieh, J. Opt. Soc. Am. B 18 (2001) 7–12.

[16] N.N. Akhmediev, A. Ankiewicz, Opt. Lett. 19 (1994) 545–547.

[17] N.N. Akhmediev, A. Ankiewicz, J.M. Soto-Crespo, Phy. Rev. Lett. 24 (1997) 4047–4051.

[18] P.F. Moulton, J. Opt. Soc. Am. B 3 (1986) 125–133.

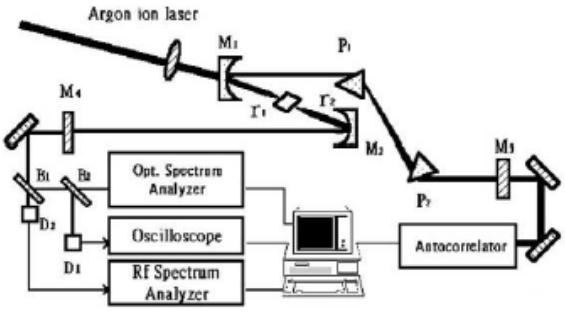


Fig. 1. Experimental setup of the Kerr-lens mode-locking Ti:sapphire laser. $B_1$, $B_2$ are beam splitter and $D_1$, $D_2$ are the high speed detectors.

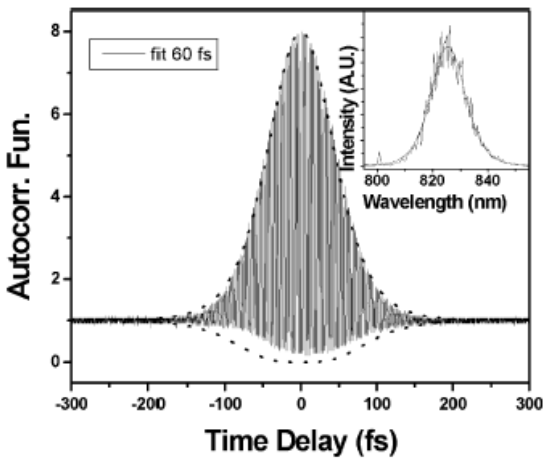


Fig. 2. Typical autocorrelation trace (solid curve) and corresponding optical-spectrum (inset) for the NML. The dash curve is fitted with the $sech^2$ function.

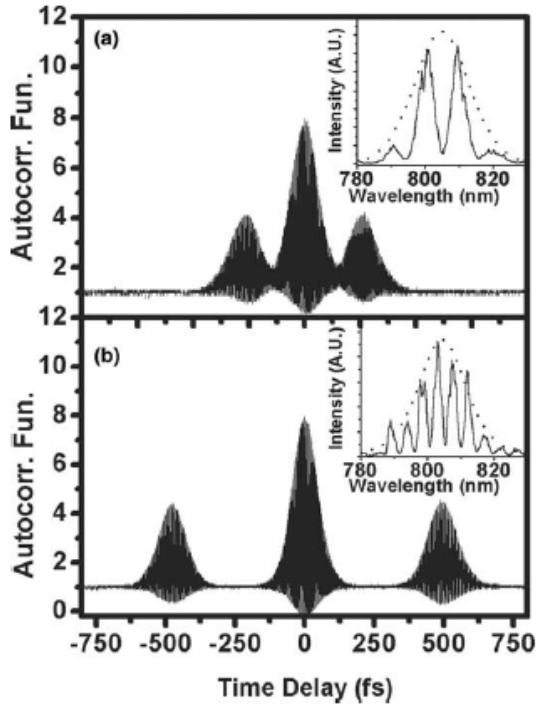


Fig. 3. Autocorrelation trace and corresponding optical-spectrum (inset) for double pulses with 210 separation as well as the relative phase $\approx \pi$ between two pulses (a), and 475 fs splitting in conjunction with $\pi/2$ phase difference in (b).

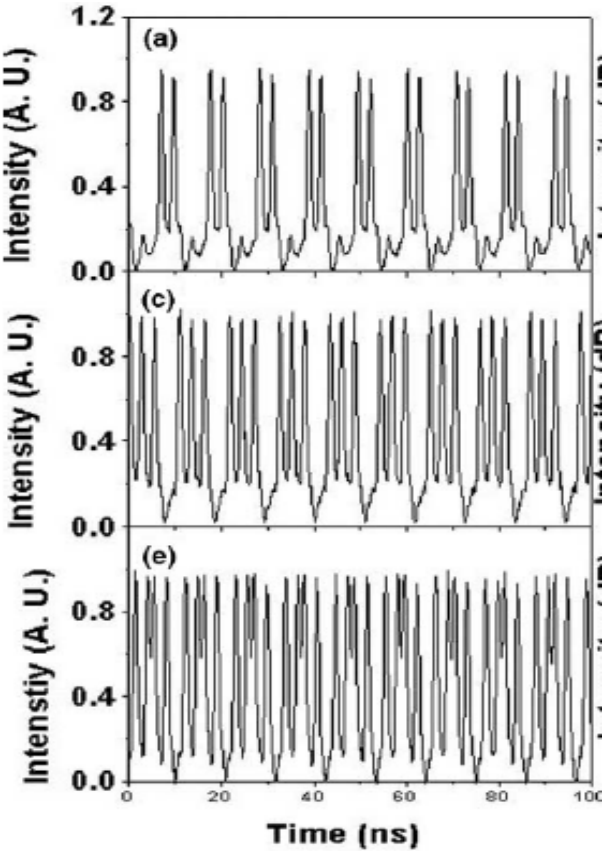


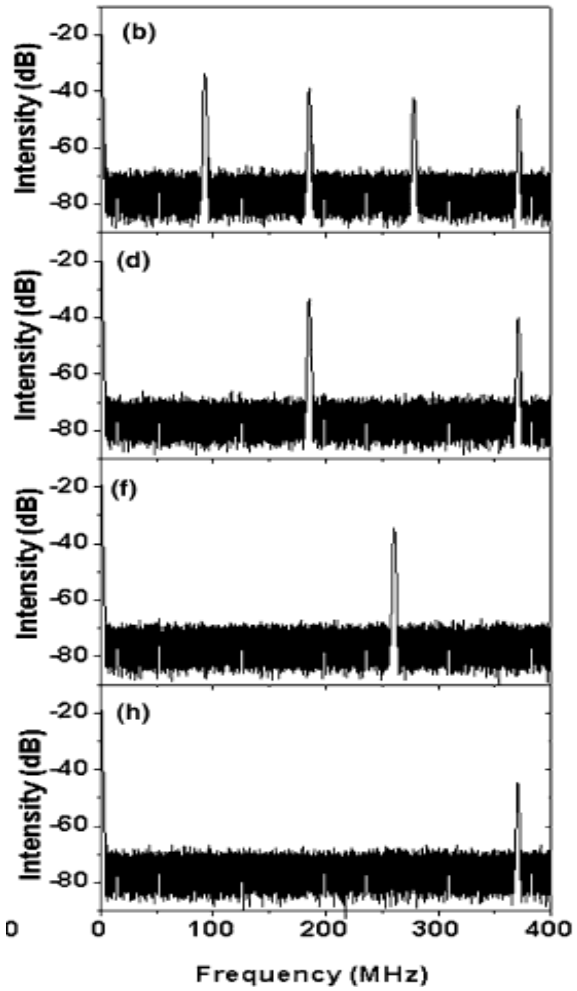


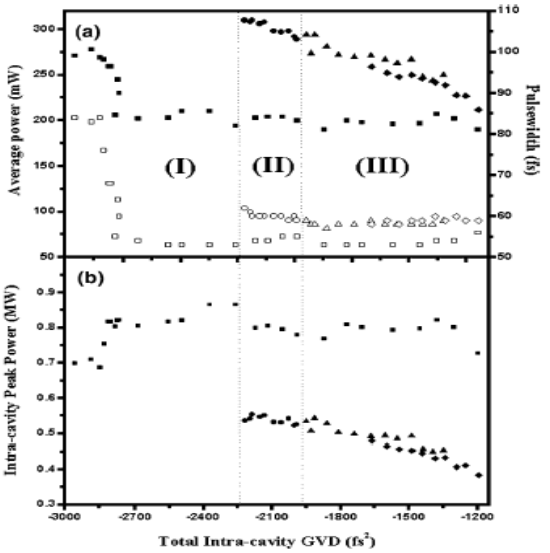


Fig. 6. The average output power (solid symbols) as well as pulsewidth (open symbols) (a) and the intra-cavity peak power; (b) versus the total intra-cavity GVD (or $\beta''$) for the NML (square), SHML (circle) and pulse-splitting states (triangle and diamond).

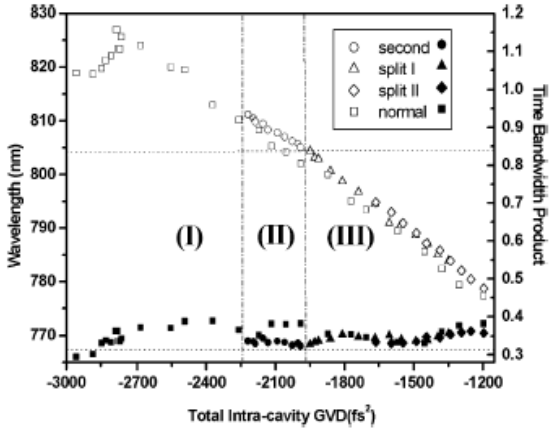


Fig. 7. The wavelength (open symbols) and time bandwidth product (solid symbols) as functions of the total intra-cavity GVD for the NML (square), SHML (circle), and pulse-splitting states (triangle and diamond).

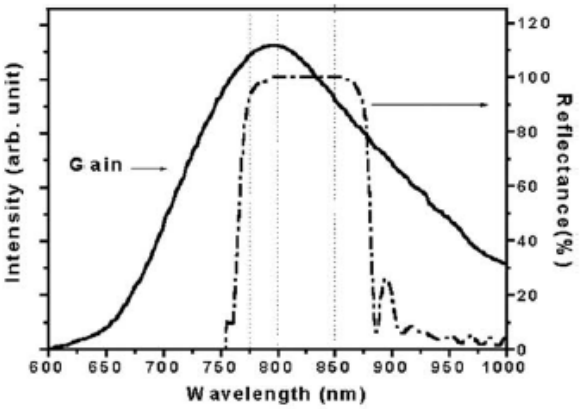


Fig. 8. The gain profile of Ti:sapphire crystal (solid line) and reflectance of curve mirrors (dashed dot line).